Mechanisms of action of therapeutic amyloidogenic hexapeptides in amelioration of inflammatory brain disease

Michael P. Kurnellas,[1] Jill M. Schartner,[2] C. Garrison Fathman,[2] Ann Jagger,[2] Lawrence Steinman,[1] and Jonathan B. Rothbard[1,2]

[1]Department of Neurology and Neurological Sciences and [2]Department of Medicine, Division of Immunology, Stanford University School of Medicine, Stanford, CA 94305

Amyloid fibrils composed of peptides as short as six amino acids are effective therapeutics for experimental autoimmune encephalomyelitis (EAE). Immunosuppression arises from at least two pathways: (1) expression of type 1 IFN by pDCs, which were induced by neutrophil extracellular traps arising from the endocytosis of the fibrils; and (2) the reduced expression of IFN-γ, TNF, and IL-6. The two independent pathways stimulated by the fibrils can act in concert to be immunosuppressive in Th1 indications, or in opposition, resulting in inflammation when Th17 T lymphocytes are predominant. The generation of type 1 IFN can be minimized by using polar, nonionizable, amyloidogenic peptides, which are effective in both Th1 and Th17 polarized EAE.

CORRESPONDENCE
Lawrence Steinman:
steinman@stanford.edu

Abbreviations used: EAE, experimental autoimmune encephalomyelitis; NET, neutrophil extracellular trap; PBC, peripheral blood cell.

Understanding the structure–function relationships of amyloid fibrils has been hindered both by their structural heterogeneity, toxicity, and insolubility in physiological buffers. The dominant structural element of all amyloid fibrils is a cross-β spine. Studies have demonstrated that amyloid fibrils can be formed by peptides as short as 5 or 6 amino acids (Nelson et al., 2005; Sawaya et al., 2007; Eisenberg and Jucker, 2012). The resultant fibrils are composed of two extended β pleated sheets, whose side chains interdigitate with those from the adjacent sheet to form a zipper interface. Fibrils formed from these relatively short peptides differ from fibrils composed of intact proteins by their structural simplicity, relative homogeneity, lack of cytotoxicity, and increased solubility in physiological buffers, thus rendering them useful for understanding how fibril structure impacts physiology. More recently, the effectiveness of amyloid-forming peptides as potential drugs has been characterized and exploited to reverse paralysis in a widely used animal model of neuroinflammation, experimental autoimmune encephalomyelitis (EAE).

We have described how amyloid fibrils composed of a variety of amyloidogenic hexapeptides are molecular chaperones. When administered to mice with EAE, the peptides reduce serological levels of IL-6 and ameliorate the paralytic clinical signs (Kurnellas et al., 2013). Peptides with the identical composition but different sequences, which were not able to form fibrils, did not inhibit insulin aggregation and amyloid formation and were not therapeutic, thus establishing that fibril formation was essential for chaperone function and therapeutic benefit (Kurnellas et al., 2013).

An important characteristic of amyloidogenic peptides is that not all the peptides form amyloid fibrils in physiological buffers at similar rates. Detailed structures of the fibrils for several of the peptides help explain the differential ability of their capacity to form fibrils in vitro (Fig. S1; Nelson et al., 2005; Sawaya et al., 2007; Eisenberg and Jucker, 2012). Peptides whose zipper interface was composed of hydrophobic amino acids rapidly form fibrils (Tau 623–628, Aβ A4 16–21, 29–34, 35–40, and 37–42). In several cases, neutralization of an ionizable amino acid (aspartic glutamic acids or lysine) allowed for fibril formation. In contrast, a set of peptides whose zipper interface was rich in polar, nonionizable amino acids (serine, threonine, asparagine, and glutamine) did not form detectable amounts of fibrils in vitro but were nevertheless

The Rockefeller University Press $30.00
J. Exp. Med. 2014 Vol. 211 No. 9 1847-1856
www.jem.org/cgi/doi/10.1084/jem.20140107

The Journal of Experimental Medicine

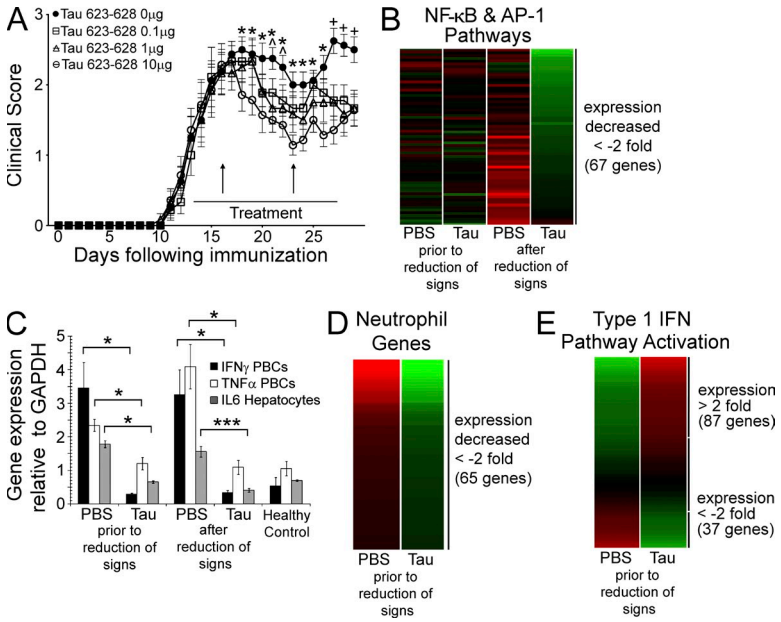

Figure 1. Effect of the injection of amyloid fibrils on gene expression in blood cells. (A) Time course of the treatment of groups of 10 mice with active EAE injected i.p. for 14 d beginning at the onset of hind limb weakness with 0, 0.1, 1, or 10 µg Tau 623–628, showing blood draws for analysis before, and after, reduction of clinical signs (vertical arrows). Values in the graph represent mean ± SEM. *, $P < 0.05$ for 10 µg; ^, $P < 0.05$ for 1 µg; and +, $P < 0.05$ for all doses by Mann-Whitney *U* test. (B) Heat map of 67 genes, induced by NF-κB and/or AP-1, whose expression decreased greater than twofold after the clinical signs of EAE were reduced but were only partially modulated before the reduction of clinical signs. Individual genes are listed in Table S1. (C) Differential gene expression measured by qPCR for IFN-γ, TNF, and IL-6 expression before and after clinical signs were reversed. Values in graph represent mean ± SEM. *, $P < 0.04$; and ***, $P < 0.005$ by Student's *t* test. Triplicates for each mouse ($n = 3$) performed in two independent experiments. (D) Heat map of 65 genes expressed in neutrophils whose expression was reduced more than twofold before visible reduction of clinical signs. Individual genes are listed in Table S2. (E) Heat map displaying the expression of 124 genes stimulated by type 1 IFN, STAT1, and/or IRF3 that were consistent with activation of these pathways before reduction of clinical signs. Individual genes are listed in Table S3.

therapeutic (Amylin 28–33 [Wiltzius et al., 2008], Apolipoprotein E 53–58, and Ig Kappa 5–10). The amyloidogenic peptides precipitated a set of plasma proteins, which included a variety of apolipoproteins, complement and coagulation proteins (Kurnellas et al., 2013), and proteins previously shown to bind amyloid fibrils such as clusterin, apolipoprotein E, complement 4 binding protein, complement factor H, and complement component C1q (Matsubara et al., 1996; Sjöberg et al., 2008; Erlich et al., 2010; Narayan et al., 2012; Calero et al., 2012; Sjölander et al., 2012). These proteins represent potential sites where in vivo fibril formation could be catalyzed.

To further examine the mode of action of amyloid fibrils, whole genome expression analysis was performed on peripheral blood cells (PBCs) isolated from mice with EAE treated with the fibrils or PBS. PBCs from mice treated with the fibrils exhibited reduction in the gene expression of TNF, IFN-γ, and IL-6, and concomitant reduction in the NF-κB and STAT3 pathways, and down-regulated networks involved in lymphocyte, monocyte, and DC activation. The fibrils also affected several genes involved in neutrophil activation and the induction of type 1 IFN. Amyloid fibrils, as nanoparticles, would be expected to be endocytosed by neutrophils, monocytes, and eosinophils (Doherty and McMahon, 2009; Sokolowski and Mandell, 2011). Previous studies have established that amyloid fibrils composed of full-length proteins stimulated neutrophils to produce neutrophil extracellular traps (NETs) and that they subsequently induced plasmacytoid DCs to produce type 1 IFN (Lande et al., 2011; Azevedo et al., 2012; Di Domizio et al., 2012).

Type 1 IFN varies in therapeutic efficacy in different models of EAE, with the cytokine being efficacious in Th1-induced disease but deleterious when the disease is induced by Th17 lymphocytes (Axtell et al., 2010, 2011, 2013). These animal models, along with IFNAR knockout animals, were used to demonstrate that two independent, therapeutic pathways exist, with the dual nature of the responses acting in concert in active and Th1-induced EAE but in opposition in Th17-induced disease. Using peptides that slowly form fibrils in vitro, the amount of type 1 IFN induced can be modulated, but equivalent molecular chaperone function is maintained, allowing peptides from this class of sequences to be therapeutically effective in both Th1- and Th17-induced EAE.

RESULTS

Gene expression modulated by amyloid fibrils

i.p. injection of amyloid fibrils modulates the paralytic clinical signs of EAE in a dose-dependent fashion (Fig. 1 A) and reduced serological levels of IL-6 (Kurnellas et al., 2013). To ask how the fibrils modulated gene expression in blood cells, the disease was induced in mice by administration of MOG 35–55 in complete Freund's adjuvant and Pertussis toxin (active EAE) and the mice were treated either with PBS or Tau 623–628 daily, beginning when the animals exhibited stage two clinical signs. Blood was collected before clinical evidence of disease (day 3 of treatment) and after clinical signs were minimized (day 10 of treatment; Fig. 1 A).

The timing of the sample collection before and after reduction of clinical signs was an attempt to identify those genes whose changes in expression would be central to the therapeutic effect and not the result of reduction of clinical signs, which might well be characterized by differential expression at the later time point. Consistent with the remission of clinical signs observed on day 10, the patterns of gene expression in PBCs from mice treated with the Tau fibrils compared with those treated with PBS were characteristic of a broad reduction of

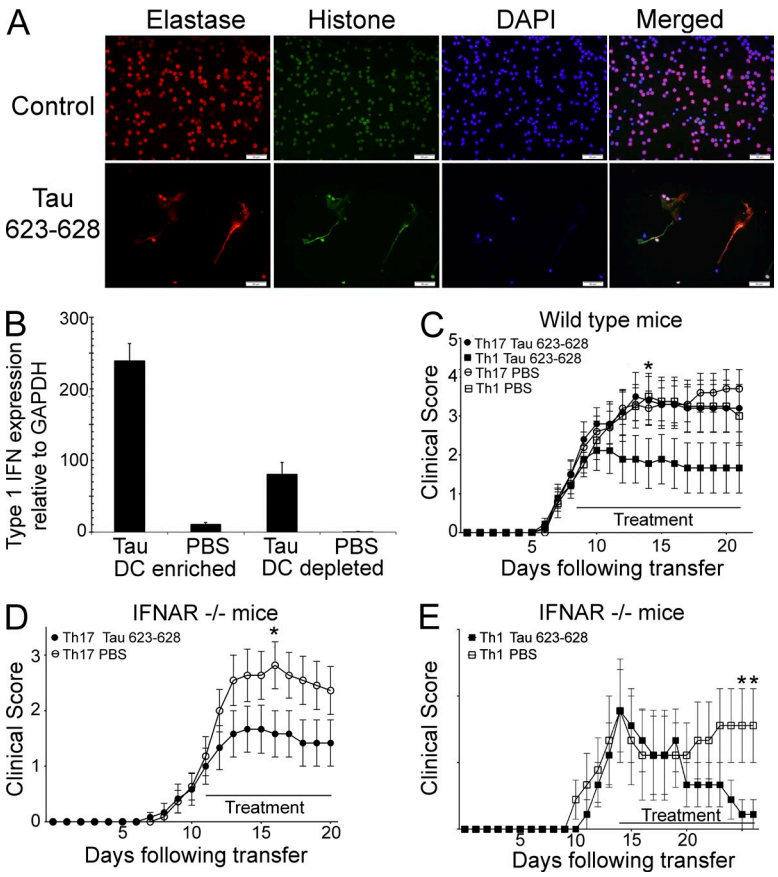

Figure 2. Amyloid fibrils composed of Tau 623–628 induce NETosis, stimulate plasmacytoid DCs to secrete type 1 IFN, and differentially affect adoptively transferred Th1 and Th17 EAE. (A) Human neutrophils were incubated with 100 ng tau 623–628 or PBS as control for 2 h. Cells were stained with anti-neutrophil elastase (red), anti-histone 3 (green), or DAPI (blue) and NETosis was determined by extracellular elastase and histone. The figures are representative of three independent experiments with an $n = 6–8$ for each condition and each experiment. Bars, 50 µm. (B) Type 1 IFN gene expression in the DC-enriched cells treated with tau 623–628 compared with PBS as measured by qPCR. Triplicates for each mouse ($n = 3$) performed in two independent experiments. (C) Adoptively transferred Th1 or Th17 cells were used to induce EAE. Groups of 10 mice were injected i.p. for 14 d beginning at onset of hind limb weakness with 10 µg Tau 623–628. (D and E) Th17 (D) and Th1 (E) lymphocytes were adoptively transferred to two groups of 10 IFNAR knockout mice, with each treated with 10 µg Tau 623–628 or PBS. Bars represent the duration of the treatment. Values in graph represent mean ± SEM. *, $P < 0.05$ by Mann-Whitney *U* test.

the inflammatory response. Pathway analysis revealed significant reductions in lymphocyte, DC, and macrophage activation, and neutrophil and phagocyte chemotaxis. The pattern of gene expression at this late time point displayed reduced activity of transcriptional factors NF-κB, AP-1, NFAT, Spl1, E2F1, and ETS1, which was not seen before the reduction of clinical signs (Fig. 1 B and Table S1).

Quantitation of the gene expression of TNF and IFN-γ in PBCs and IL-6 in hepatocytes, as measured by qPCR, were at normal levels not only when the clinical signs were reduced but also before reduction of the clinical signs on day 3 (Fig. 1 C), indicating that their reduced expression might well be a central factor in the abrogation of the disease. Only the reduction of IL-6 was seen when the proteins were measured in the plasma of treated animals (Kurnellas et al., 2013).

Analysis of gene expression before reduction of clinical signs revealed two additional patterns: (1) increased expression of the genes involved in the TLR and MYD88 pathway, along with the reduction in the expression of neutrophil related genes; and (2) a clear pattern for the induction of type 1 IFN pathway (Fig. 1, D and E; and Tables S2 and S3). Expression of IFN-α4, 5, 9, 12, 13, and IFN-β were all significantly increased by day 3 of treatment before the modulation of clinical signs, which was supported by the change in expression of 124 known type 1 IFN-inducible genes including Oas1, 2, Isg15, Mx1, Rsad2, Herc5, Aqp3, and Ifit1, Ifit3, and IRF1 (Table S3).

Differential effects of treatment with Tau 623–628 on EAE induced by T lymphocyte adoptive transfer

The induction of type 1 IFN by the injection of amyloid fibrils has been documented in previous studies where fibrils composed of full-length proteins induced neutrophil NETosis, which in turn were capable of activating plasmacytoid DCs through TLR and MYD88 pathways to secrete the cytokines (Lande et al., 2011; Azevedo et al., 2012; Di Domizio et al., 2012). Consistent with these published studies, fibrils composed of Tau 623–628 induced NETs when incubated with purified neutrophils, and when injected into mice stimulated type 1 IFN in samples enriched in plasmacytoid DCs (Fig. 2, A and B).

Type 1 IFN production also could explain the immunosuppressive effects of the fibrils because IFN-β is an effective therapeutic for active EAE and multiple sclerosis (Arnason, 1999). However, recent studies have established that type 1 IFN exhibits dual activities, inhibiting inflammation when there is a predominance of Th1 lymphocytes and enhancing the inflammatory pathologies of diseases dominated by Th17 lymphocytes, which include Sjögren's syndrome, systemic lupus erythematosus, neuromyelitis optica, rheumatoid arthritis, and psoriasis (Axtell et al., 2010; Axtell and Raman, 2012). The differential activity of this family of cytokines can be used in this setting to test the relative importance of type 1 IFN induction by the amyloid fibrils in vivo using animal models of EAE in which the disease was induced by adoptive transfer of either Th1 or

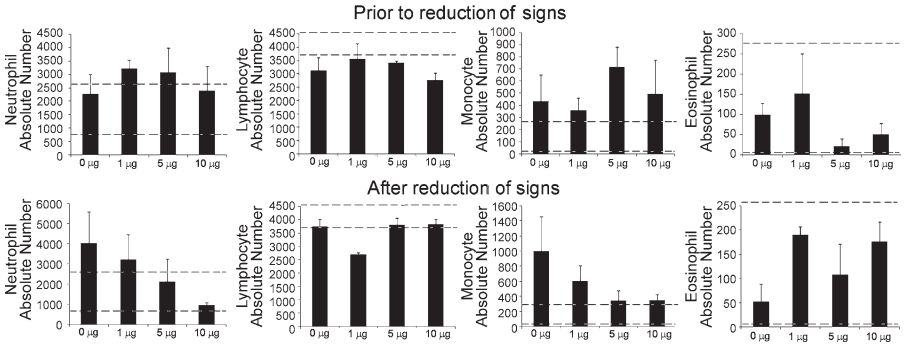

Figure 3. Repeated administration of fibrils derived from Tau peptide result in a dose-dependent reduction of the number of neutrophils and monocytes in peripheral blood. The total number of neutrophils, lymphocytes, monocytes, and eosinophils were quantified from mouse blood during active EAE. Tau 623–628 was administered at 0, 1, 5, and 10 μg daily and blood was collected before changes in clinical score (3 treatments) or after the reduction of clinical signs (7 treatments). The normal ranges of the number of cells in healthy mice are indicated between the dashed lines. A single CBC analysis was performed for all groups (n = 3). Values in graph represent mean ± SEM.

Th17 lymphocytes. If type I IFN is stimulated by the amyloid fibrils at levels that are physiologically relevant, then the peptides should be effective therapeutics in Th1-induced but not Th17-induced disease.

As expected, daily injection of the fibrils (10 μg/d), beginning on the day of stage 2 disease, resulted in a reduction of clinical signs in mice whose disease was induced with lymphocytes with an enhanced number of Th1 cells but not in mice injected with predominantly Th17 cells (Fig. 2 C). Interestingly, the signs of EAE in the mice induced with Th17 lymphocytes were not exacerbated as would be expected by the treatment with IFN-β. Rather, the clinical signs were equivalent to mice treated with PBS, which could be due to the fibrils inducing a second anti-inflammatory mechanism based on their activity as molecular chaperones. In this model, the immune modulatory chaperone activity would act in concert with type I IFN effects in animals with active EAE or Th1-induced disease but would counteract the effects of type 1 IFN in EAE induced with Th17 lymphocytes. Experimental confirmation of this model was observed when Th17- and Th1-mediated EAE were induced in IFNAR knockout animals who were treated with Tau 623–628. Without the capability of activating the type 1 IFN pathway in these animals, administration of the Tau fibrils reduced the paralytic clinical signs, demonstrating that type 1 IFN activation was proinflammatory in Th17 adoptive transferred EAE, and that the amyloid fibrils induced a second, independent anti-inflammatory, therapeutic pathway (Fig. 2, D and E).

We realized that if the fibrils were inducing NETosis, then the circulating neutrophil population could be affected, which if reduced could explain the decrease in expression of a set of neutrophil genes (Fig. 1 D). Measurement of the complete blood cell count from mice with active EAE, treated before or after reduction of clinical signs with varying doses of Tau ranging from 0 to 10 μg (0–32 nM), revealed that both neutrophil and monocyte numbers were reduced in a dose-dependent fashion in mice after modulation of the clinical signs but not before (Fig. 3). The number of eosinophils increased, whereas the number of lymphocytes was unaffected. The effects were not due to the toxicity of fibrils because in contrast to Aβ 1–40 and 1–42, which resulted in significant toxicity of human monocytes at 10 μM and complete lysis at 100 μM, incubation with fibrils composed of L- or D-Tau 623–628 at 100 μM for 9 h exhibited minimal cellular cytotoxicity and no detectable inflammasome activation (Fig. 4).

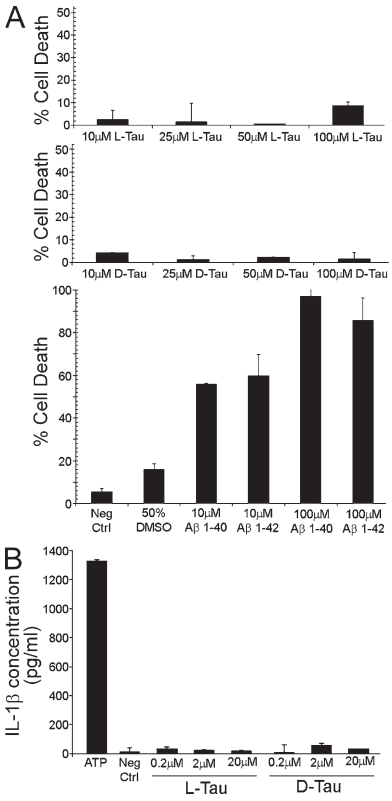

Figure 4. Amyloid fibrils composed of hexapeptides are significantly less toxic to human monocytes than fibrils composed of Aβ 1–40 or 1–42 and do not activate inflammasomes. (A) Purified human monocytes were incubated for 6 h with varying concentrations of fibrils composed of Tau 623–628 or the amyloid β (Aβ) sequences 1–40 and 1–42. The cells were isolated and cytotoxicity was measured by dye exclusion. (B) The peptides did not induce detectable levels of IL-1β. Two independent experiments were performed on triplicates for each condition (n = 3). Values in graph represent mean ± SEM.

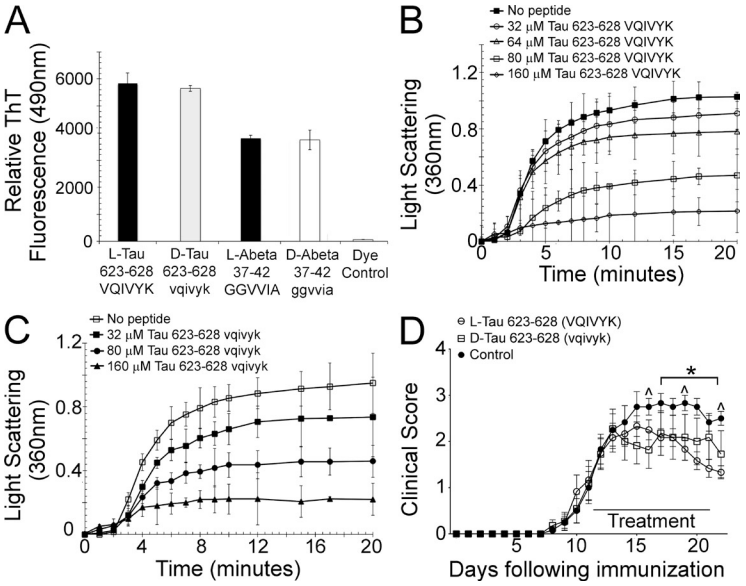

Figure 5. Tau 623–628 composed of L- or D-amino acids formed amyloid fibrils equivalently and were equally effective molecular chaperones with similar therapeutic efficacies. (A) L- and D-Tau 623–628 and L- and D-Aβ 37–42 (200 µg/50 µl) were each added to 140 µl of 10 µM MES, pH 7.4, and incubated at 37°C for 5 min. ThT (10 µl of 10 µM solution) was added and the resultant fluorescence at 490 nm from excitation at 440 nm was measured using a fluorescent plate reader. The levels of ThT were similar in both sets of hexapeptides. (B and C) L-Tau (B) and D-Tau (C) 623–628 inhibit insulin aggregation (170 µM) in a dose-dependent manner with similar IC_{50} concentrations. The ThT and chaperone assays were done in triplicate ($n = 3$) and repeated twice. (D) Groups of 10 mice with active EAE were injected daily i.p. for 10 d with 1 µg L-Tau or D-Tau hexapeptides beginning at onset of hind limb weakness. PBS was injected in littermates as control. Bars represent the duration of the treatment. The graphs are representative of 2 independent experiments and values in graph represent mean ± SEM. *, $P < 0.05$ for L-Tau; and ^, $P < 0.05$ for D-Tau by Mann-Whitney *U* test.

Therapeutic effect of the amyloid fibrils does not involve stereospecific cell surface receptor

The types of blood cells whose populations were most affected by administrations of the fibrils were those known to endocytose particles, such as insoluble amyloid fibrils (Doherty and McMahon, 2009; Sokolowski and Mandell, 2011). As particles, the fibrils could be endocytosed in a receptor-dependent or -independent fashion, which can be tested by determining whether stereoisomeric fibrils composed of D-amino acids were equally effective. Amyloidogenic peptides composed of either D- or L-amino acids should form β pleated sheets equivalently and also assemble equally into amyloid fibrils. However, whether the resultant fibrils would be able to be equivalent molecular chaperones and therapeutic agents is unclear. To test this hypothesis, Tau 623–628 (Ac vqivyk CONH2) and Aβ 35–40 (Ac mvggvv CONH2) composed of D-amino acids were compared with the peptides composed of L-amino acids for their ability to form amyloid fibrils and were shown to be equivalent, within error, as defined by staining with Thioflavin T (Fig. 5 A). The resultant stereoisomeric fibrils composed of the L- or D-Tau peptide also inhibited aggregation of a solution of 170 µM insulin with an equivalent IC_{50} value of ∼75 µM (Fig. 5, B and C). When used as therapeutic agents for EAE, equal reduction of paralytic signs by the two isomers was observed (Fig. 5 D). The therapeutic equivalence of the two isomeric peptides indicates that their mode of action will not be dependent on their binding by a stereoselective receptor and that proteolytic cleavage of the peptides does not appear to be a major factor in limiting their mode of action.

Variation in the induction of type 1 IFN by different amyloidogenic peptides

Even though the production of type 1 IFN has been shown to be beneficial in diseases in which the Th1 phenotype predominates, the cytokine, as has been shown in this model, can exacerbate Th17-based diseases. Type 1 IFN potently differentiates monocytes, matures DCs, promotes B cell differentiation and antibody production, modulates survival, proliferation, and differentiation of T cells, and primes neutrophils for death by NETosis (Axtell and Raman, 2012). Therefore, an amyloid fibril that minimally stimulates type 1 IFN production might be a better therapeutic design.

Analysis of the physical properties of the original set of 20 amyloidogenic peptides (Fig. S1) revealed that a set of polar, nonionizable sequences failed to form ThT staining fibrils in vitro, even at 2 mg/ml in physiological buffers for >8 wk. Nevertheless, when assayed for therapeutic benefit in active EAE, these peptides were equally potent as the peptides that readily formed fibrils in vitro, indicating that the peptides form fibrils in serum at sufficient levels to become therapeutic.

To determine whether they induce equivalent amounts of type 1 IFN as a peptide that rapidly forms fibrils, such as Tau 623–628, healthy C57BL/6 mice received two daily i.p. injections of 10 µg Amylin 28–33 or Tau 623–628 and bled on the third day. RNA was isolated from PBCs, converted into cDNA, and the amount of type 1 IFN was measured by qPCR using specific primers for murine IFN-α4, 5, 12, and 13, as well as a set of consensus primers (Hahm et al., 2005). As measured by both the individual and consensus primers, the polar Amylin peptide induced approximately half the amount of type 1 IFN as the Tau peptide (Fig. 6, A and B), which confirms indirectly the formation of Amylin fibrils in vivo.

Previous experiments established that polar, nonionizable peptides were equally therapeutic in active EAE as peptides that readily formed fibrils in vitro, emphasizing that the molecular chaperone function appears to be central to therapy (Kurnellas et al., 2013). Mice induced with Th17 lymphocytes were treated daily with 2 µg of the Amylin peptide beginning the day after adoptive transfer of the disease. Unlike animals treated with the preformed Tau fibrils, treatment with monomeric Amylin peptide reduced the clinical signs to a statistically significant level, confirming that the pleotropic effects of type 1 IFN induction

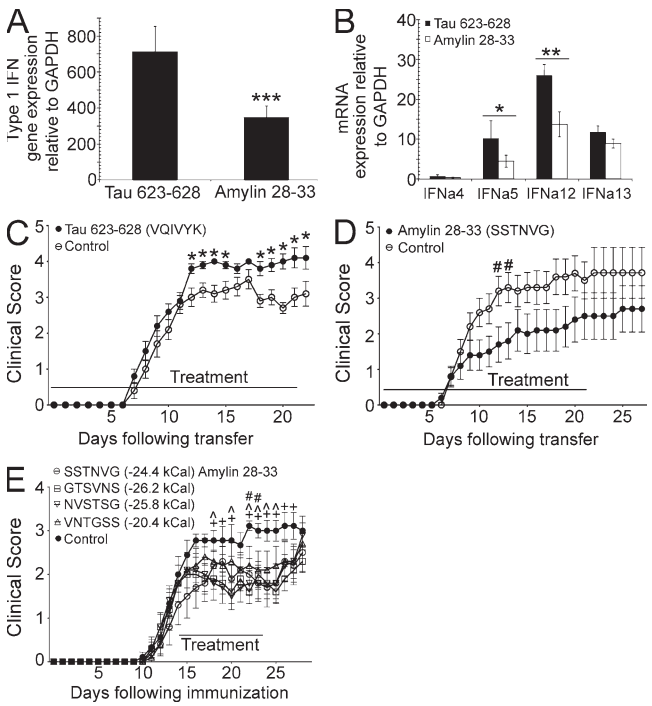

Figure 6. A polar, amyloidogenic peptide, Amylin 28–33, induces a fraction of the type 1 IFN as Tau 623–628 and is therapeutic in Th17-induced EAE. (A and B) Quantification of type 1 IFN induced in PBCs from sets of five C57BL/6 mice after three injections of 10 µg of either Amylin 28–33 or Tau 623–628 using qPCR with consensus primers for type 1 IFN (A) or primers for IFN-α4, 5, 12, and 13 (B). Two independent experiments were performed and the values in graph represent mean ± SEM. *, P < 0.02; **, P < 0.002; and ***, P < 0.0002 by Student's *t* test. (C and D) Plot of clinical signs of groups of 10 mice with EAE was induced on day 0 by adoptive transfer of Th17 lymphocytes that were treated with 2 µg Tau 623–628, Amylin 28–33, or PBS daily for 21 d. (E) Groups of 10 mice with active EAE were treated for 10 d with 10 µg Amylin 28–33 or shuffled sequences of Amylin 28–33 with lower and higher Rosetta free energies. Values in graph represent mean ± SEM. *, P < 0.05 for VQIVYK; #, P < 0.05 for SSTNVG; +, P < 0.05 for GTSVNS; and ^, P < 0.05 for NVSTSG by Mann-Whitney *U* test.

can overcome the anti-inflammatory effects of the molecular chaperones in this model (Fig. 6, C and D).

A simple shuffled peptide acting as a negative control for this experiment was not easily identified because the five different amino acids of the sequence all exhibit high β sheet propensity and are compatible with the zipper interface. Three analogues of the Amylin sequence, SSTNVG, were synthesized, with two corresponding to sequences with lower Rosetta free energy than the natural sequence (greater amyloid propensity; Goldschmidt et al., 2010; López De La Paz et al., 2002), GTSVNS and NVSTSG, and one with a higher free energy, VNTGSS. When used as therapeutic agents for EAE, all three peptides appeared to reduce the clinical signs relative to the untreated control with the rank hierarchy of the amelioration of signs correlating with the predicted amyloidogenicity. Statistically significant reduction of signs was observed only with the natural sequence and the two peptides with lower Rosetta free energy than amylin. Statistically significant reduction of the paralytic signs was not observed for the shuffled peptide predicted to be less amyloidogenic (Fig. 6 E), supporting the premise that the therapeutic effects of the polar peptides arise from the formation of amyloid fibrils in vivo.

DISCUSSION

The experimental data presented here support a model where administration of amyloid fibrils composed of hexapeptides stimulates two separate pathways that contribute to their therapeutic properties. As molecular chaperones, the fibrils reduce IL-6, TNF, and IFN-γ and resultant inflammation, which we speculate is caused by the inhibition of the formation of aggregates, or amyloid fibrils, of plasma proteins. The second pathway is the induction of type 1 IFN, which can either act in concert with, or counteract, the chaperone activity to limit the signs of EAE depending on whether the disease is dominated by Th1 or Th17 lymphocytes (Fig. S2). The amyloid fibrils composed of Tau 623–628 have limited solubility in physiological buffers and, consequently, as particles are phagocytosed based on differential gene expression, most prominently by neutrophils soon after i.p. injection. The fibrils induce neutrophils to undergo NETosis, reducing their numbers in blood and inducing plasmacytoid DCs to secrete type 1 IFN, consistent with previous studies in animal models of lupus (Lande et al., 2011; Azevedo et al., 2012; Di Domizio et al., 2012).

Analysis of the differential gene expression induced after three treatments with the fibrils, before reduction of the clinical signs of EAE, revealed that a set of type 1 IFN genes and a spectrum of genes in the type 1 IFN pathway were induced. The induction of the cytokine was shown to be an important factor in therapeutic activity of the fibrils. Consistent with previous experiments with injection of type 1 IFN, treatment with preformed Tau fibrils was therapeutic in EAE induced by Th1 cells but was ineffective or exacerbated the paralytic clinical signs in mice whose disease was induced by Th17 lymphocytes, depending on the duration and amount of the fibrils administered (Figs. 2 and 6; Axtell et al., 2011). Injecting the Tau fibrils into mice whose type 1 IFN receptors were not expressed diminished signs of disease, demonstrating that if type 1 IFN pathways were inhibited, then the fibrils were beneficial in EAE induced by Th17 lymphocytes, thus establishing the presence of a second therapeutic pathway.

Both of the proposed pathways—induction of neutrophils to produce nets, leading to the induction of type 1 IFN, and the reduction of proinflammatory protein aggregates—do not involve chiral receptors; thus, fibrils composed of D-amino acids would be expected to be equally active as their stereoisomers, consistent with the experimental data. The biological equivalence of fibrils composed of D- and L-amino acids still would allow mechanisms wherein the fibril is bound by a plasma protein—for example clusterin, which is itself part of HDL—and the fibril enters cells via the stereoselective HDL receptor. The data in this paper postulate that the modes of action of

the fibril do not arise from a direct chiral interaction with a cell surface receptor.

The fibrils composed of the Tau peptide have proven useful in exploring the biological activities of the amyloid fibrils. However, injection of any particle, regardless of size, would be problematic in translating these peptides to human therapeutics. The dynamics of amyloid fibril formation is an additional complication in the difficulty of formulating samples of the Tau peptide in physiological buffers that contain equal, and reproducible, amounts of fibrils. Normalization by staining with thioflavin T is a relatively crude measure of fibril content and does not consider the distribution of fibrils of different length. Finally, the induction of type 1 IFN is beneficial in active EAE but certainly is problematic in diseases with a Th17 signature.

The search for an alternative amyloidogenic peptide as a possible therapeutic focused on those sequences that formed fibrils more slowly in vitro due to their polar zipper interfaces, for example, Amylin 28–33, Ig Kappa 5–10, and Apolipoprotein E 53–58 (Fig. S1). The fact that these sequences do not readily form fibrils in physiological buffers is consistent with their lack of a hydrophobic character at the zipper interface. Nevertheless, these amyloidogenic peptides were therapeutic and, most importantly, stimulated significantly less type 1 IFN production, which is dependent on fibril formation. An important caveat is that measurement of fibrils by ThT is relatively insensitive, requiring high micromolar concentrations, and is an important technical limitation of measuring small amount of amyloid fibrils. The polar peptides form fibrils more slowly than amyloidogenic sequences whose association are driven by hydrophobic forces and would not be expected to be phagocytosed as readily. Fibril formation also might not be immediate, allowing the peptides to bypass neutrophils in the peritoneum and form when associated with monocytes (Sheedy et al., 2013) or plasma proteins known to bind amyloid fibrils, such as apolipoprotein E, complement C1q, clusterin, and complement factor H. The importance of these potential interactions can be studied in animals unable to express these proteins and using direct biochemical measurements, which can be studied more readily using the hexapeptides than insoluble protein aggregates.

These experiments demonstrate that through understanding the modes of action of the fibrils, the structures of the composite peptides can be modified to modulate their biological activity. This correlation of structure and function is an effective method to identify an optimal clinical candidate. The amyloidogenic peptides with polar zipper interfaces have several attractive features as potential drug candidates. Their synthesis is relatively rapid and inexpensive and they are freely soluble in physiological buffers. The peptides slowly aggregate in aqueous solution and can be delivered with osmotic pumps without concern of blockage, and yet they self-assemble into biologically active nanoparticles capable of modulating both the innate and adaptive immune responses.

The induction of type 1 IFN by preformed amyloid fibrils composed of the Tau peptide leads to the question of whether there are examples of other particles in the literature being therapeutic for EAE. An interesting possibility is in the therapeutic benefit shown by the administration of uric acid (Scott et al., 2002). Crystals of uric acid have been shown to be endocytosed and induce inflammasomes with subsequent secretion of IL-1β by monocytes. The data in this paper would predict that their therapeutic benefit would arise from their endocytosis by neutrophils with resultant stimulation of type 1 IFN. A second example is the remarkable fact that mice engineered to prevent the expression of a prominent amyloidogenic protein exhibit greater paralytic signs when active EAE is induced. This has been reported for knockouts of amyloid precursor protein (Grant et al., 2012), major prion protein (Gourdain et al., 2012), tau (Weinger et al., 2012), serum amyloid P (Ji et al., 2012), and αB crystallin (Ousman et al., 2007). A possible explanation for this pattern is that each of these proteins is forming levels of amyloid fibrils that induce type 1 IFN production, which would modulate the clinical signs of EAE. Removal of the protein expression would negatively affect the disease course.

Reduction of IL-6, IFN-γ, and TNF before reduction of paralysis is noteworthy and distinguishes their therapeutic activity from both anti-TNF and anti–IL-6 receptor antibodies because the fibrils appear to exhibit a broader immunosuppressive function than the individual antibodies. Anti–IL-6 receptor antibodies are prophylactic and not therapeutic in EAE (Serada et al., 2008), likely because the antibody does not target multiple pathways simultaneously. Similarly, anti-TNF selectively modulates the NF-κB pathway but does not directly affect the STAT-1 or STAT-3 signaling pathways. Interestingly, combination therapies, which would better reflect the effects of the fibrils, have demonstrated increased risk of infection with limited therapeutic efficacy in animal models of autoimmune disease.

Modulation of the expression of the three proinflammatory cytokines raises the question whether administration of the fibrils results in changes in a single cytokine that then subsequently affects the expression of the others, or whether the fibrils simultaneously impact multiple immunological pathways. Experiments designed to answer these questions will be important both for increased understanding of optimizing the lead peptide and to understand further how amyloid fibrils can modulate the immune system.

MATERIALS AND METHODS

Induction of active EAE in mice by immunization with MOG and adjuvant. EAE was induced by procedures previously described in female wild-type C57BL/6J mice (The Jackson Laboratory) or IFN-α/β receptor (IFNAR)–deficient mice backcrossed for 10–12 generations on a C57BL/6 background (obtained from C. Raman, University of Alabama at Birmingham, Birmingham, AL). In brief, EAE was induced at 9 wk of age by subcutaneous immunization in the flank with an emulsion containing 200 µg myelin oligodendrocyte glycoprotein$_{35-55}$ (MOG35-55; MEVGWYRSPFSRVVHLYRNGK) in saline and an equal volume of complete Freund's adjuvant containing 4 µg/ml mycobacterium tuberculosis H37RA (Difco Laboratories). All mice were administered 400 ng pertussis toxin (List Biological) i.p. at 0 and 48 h after immunization. The neurological impairment was scored as follows: 0, no clinical disease; 1, tail weakness; 2, hind limb weakness; 3, complete hind limb paralysis; 4, hind limb paralysis and some forelimb weakness; 5, moribund or dead. When animals exhibited a mean of level two for clinical signs, they were injected in the peritoneum with 0.1, 1, or 10 µg Tau 623–628 peptide, or PBS daily. All animal protocols were approved by

the Institutional Animal Care and Use Committee. Normal murine plasma was taken from age-matched healthy C57BL/6J mice.

Disease induction by adoptive transfer of Th1 or Th17 lymphocytes. 10 d after induction of active EAE, the spleen and draining lymph nodes were isolated and restimulated for 3 d with 10 µg/ml MOG_{35-55} in the presence of 10 ng/ml IL-23 for Th17 EAE or 10 ng/ml IL-12 for Th1 EAE. Lymphocytes, 15×10^6 cells per mouse, were injected i.p. into 9-wk-old female recipient C57BL/6J mice or IFNAR-deficient mice. Mice were examined daily for clinical signs of EAE and were scored on a five point scale as previously described. Atypical EAE was also scored as follows: 0, no clinical disease; 1, slight head turn with ataxia (no tail weakness); 2, more severe head turn; 3, abnormal gait and unable to walk in straight line; 4, laying on side or rolling; 5, moribund or dead. Animals were treated by i.p. injection with 2 or 10 µg Tau 623–628 or Amylin 28–33 peptide at onset of induction of disease or when mice exhibited hind limb weakness.

Peptide synthesis. Peptides were synthesized using solid phase techniques and commercially available Fmoc amino acids, resins, and reagents (PE Biosystems and Bache) on a 433A peptide synthesizer (Applied Biosystems) as previously described (Wender et al., 2000). Purity of the peptides was shown to be >90% using a 700E HPLC (PE Biosystems) and a reverse phase column (Alltech Altima). The molecular weight of the peptides was confirmed using matrix assisted laser desorption mass spectrometry.

Chaperone assays. The capacity of the proteins and peptides to inhibit DTT-induced aggregation of the β chain of insulin was assayed using procedures described previously (Hong and Fink, 2005; Hong et al., 2006). In brief, 150 µg human insulin (Sigma-Aldrich) dissolved in 100 mM NaCl and 20 mM Tris, pH 7.4, with or without varying concentration of the peptides in a total volume of 380 µl and incubated at 37°C. DTT, 20 µl of a 100 mM stock solution, was added at time zero, and the aggregation was measured by the increase in absorption at 360 nm as a function of time over 20 min. Inhibition of amyloid fibril formation was monitored by the addition of ThT (10 µl of a 10 µM solution), and the resultant fluorescence at 485 nm from excitation at 440 nm was measured using a SpectraMax 190 (Molecular Devices) fluorescent microtiter plate reader.

Thioflavin T binding. The relative amount of amyloid present in each solution was measured by combining solutions of the hexapeptides (200 µg, 50 µl) with 100 µl of 100 mM MES, pH 7.4, and 50 µl of 1 M solution of at the appropriate pH and incubated at 37°C in a black 96-well microtiter plate. ThT (10 µl of a 10 µM solution) was added and the resultant fluorescence at 485 nm from excitation at 440 nm was measured using a SpectraMax 190 fluorescent microtiter plate reader.

RNA isolation, chip hybridization, and qPCR. Total RNA was extracted from various cells and tissues using TRIZOL reagent and the RNeasy mini kit or micro kit (QIAGEN). First-strand cDNA was synthesized with 3.5–5.0 µg of total RNA using Superscript III first strand synthesis SuperMix for quantitative RT-PCR (qRT-PCR). qPCR was performed to measure mouse IFN-α, TNF, and IL-6 mRNA levels. qPCR assays were performed using the 7900HT Fast Real Time PCR System (Applied Biosystems), and the TaqMan Gene Expression Arrays (Applied Biosystems) using commercially available primers for the three cytokines and IFN-α4, 5, 12, and 13 (ABI). Consensus primers for IFN-α were those previously reported by Hahm et al. (2005). All assays were performed according to manufacturer's instructions. The comparative Ct method for relative quantification (ΔΔCt) was used to compare gene expression. Housekeeping gene expression was used to normalize expression using the following equation: normalized expression = $2^{[Ct\ (house\text{-}keeping\ gene)\ -\ Ct\ (gene)]}$. RNA was obtained from mouse blood samples whose red blood cells were lysed before freezing, and digested liver using RNeasy Mini kit (QIAGEN). RNA quality was shown to be suitable for microarray experiments (2100 Bioanalyzer; Agilent Technologies).

Gene expression changes associated with Tau treatment were quantified using a microarray (SurePrint G3 Mouse; Agilent Technologies). Analysis and quantitation of the data were done using GeneSpring and Ingenuity software.

Complete blood count (CBC). 200 µl of whole blood from mice with active EAE after 3 or 7 i.p. injections of 0, 1, 5, or 10 µg Tau 623–628 (VQIVYK) were collected into tubes containing 2 mg/ml EDTA. The CBC quantification was performed by the Stanford University Department of Comparative Medicine and included assessment of the following: white blood cells, red blood cells, hemoglobin, hematocrit, mean corpuscular volume, mean corpuscular hemoglobin, mean corpuscular hemoglobin concentration, platelet estimate, neutrophils, lymphocytes, monocytes, eosinophils, and basophils.

Toxicity assays and inflammasome activation. Human PBMCs were collected from healthy, adult volunteers under an IRB protocol approved by the Stanford Institutional review board. Using gradient centrifugation, monocytes were purified by plastic adherence overnight. Nonadherent cells were removed and fresh media (RPMI 1460 P/S/G and 10% FCS) were added to the cells. Monocytes were stimulated with 100 ng/ml LPS (Sigma-Aldrich) at t = 0, followed by L Tau, D Tau (both at 10, 25, 50, and 100 µM), Aβ-1-40, Aβ1-42 (both dissolved in 100% DMSO at 10 and 100 µM), 5 mM ATP, or 50% DMSO control at t = 3 h. Monocytes were removed by scraping at t = 9 h and stained with trypan blue. Cell death was calculated as the percentage of trypan blue–positive cells over the total number of cells. Supernatants were collected before the removal of the monocytes and IL-1β levels were measured by ELISA.

NET assay. Human neutrophils were isolated from whole blood of healthy donors in vacutainers (BD) containing sodium heparin. In brief, blood was layered onto Ficoll gradient, centrifuged at 400 *g* for 30 min, and the RBC and granulocyte layer was collected and resuspended with an equal volume of 3% dextran solution. After sedimentation for 30 min, the neutrophil-rich supernatant was collected and the remaining RBCs were lysed using ACK buffer. Neutrophils were cultured at 5×10^5 cells per well of a 24-well plate on poly-L-lysine–coated coverslips (BD) for 2 h in RPMI 1640 media supplemented with 10% fetal bovine serum, 2 mM L-glutamine, 1 mM sodium pyruvate, 0.1 mM nonessential amino acids, 100 U/ml penicillin streptomycin, and 0.5 µM 2-mercaptoethanol. Neutrophils were incubated with 100 ng/well of Tau 623–628 or PBS as control.

NETs were assessed by fluorescence microscopy using DAPI staining of cell nuclei, mouse anti-neutrophil elastase (Abcam) at 1:500 for determination of neutrophil purity, and rabbit anti-histone 3 (Millipore) at 1:500 to determine extracellular DNA indicative of NET formation. Donkey anti–rabbit FITC and donkey anti–mouse Cy3 (Jackson ImmunoResearch Laboratories, Inc.) were incubated at 1:200. The number of NETs was counted in 25 fields per coverslip at 40× magnification using a microscope (BX41; Olympus) with cellSens digital imaging software.

Plasmacytoid DC isolation. Wild-type C57BL/6 mice were injected with 10 µg Tau 623–628, Amylin 28–33, or PBS daily for 3 d. Whole blood was collected in tubes containing sodium heparin and RBCs were lysed using ACK buffer. The pDCs were isolated using an isolation kit (Miltenyi Biotec) and the percentage of cells was determined using FACs analysis with anti–mouse Ly-6C and anti–mouse CD317 antibodies (eBioscience).

Online supplemental material. Fig. S1shows hexameric, amyloidogenic peptides segregated by composition and their propensity to form fibrils. Fig. S2 shows a schematic depiction of the relationship between the two pathways that are induced by the amyloid fibrils composed of the hexapeptides. Table S1 shows that NF-κB and AP-1 pathways are inhibited when symptoms of EAE are reduced. Table S2 shows that expression of a set of neutrophil genes is inhibited before reduction of symptoms. Table S3 shows gene expression patterns consistent with activation of type 1 IFN pathway before reduction of symptoms. Online supplemental material is available at http://www.jem.org/cgi/content/full/jem.20140107/DC1.

M.P. Kurnellas was supported by a postdoctoral fellowship from a National Institutes of Health Training Fellowship (T32 AI07290-27). We gratefully acknowledge funding from the National Institutes of Health (R01NS55997 to L. Steinman, U01DK078123 to J.B. Rothbard, and 1R43AI0949 to J.B. Rothbard and L. Steinman). This work was supported by the National MS Society (to J.B. Rothbard and L. Steinman) and the Endriz Fund (to L. Steinman).

The authors declare no competing financial interests.

Author contributions: M.P. Kurnellas performed all the animal experiments establishing the therapeutic activity and differential activity of the peptides and measured the ability of the peptides to stimulate neutrophil NETosis, J.B. Rothbard performed the molecular chaperone assays, the gene expression, and qPCR experiments with J.M. Schartner, A. Jagger purified the monocytes and performed the inflammasome and cytotoxicity assays. C. Garrison Fathman and L. Steinman oversaw all aspects of the research and wrote the paper with J.B. Rothbard and M.P. Kurnellas.

Submitted: 16 January 2014
Accepted: 2 July 2014

REFERENCES

Arnason, B.G.W. 1999. Immunologic therapy of multiple sclerosis. *Annu. Rev. Med.* 50:291–302. http://dx.doi.org/10.1146/annurev.med.50.1.291

Axtell, R.C., and C. Raman. 2012. Janus-like effects of type I interferon in autoimmune diseases. *Immunol. Rev.* 248:23–35. http://dx.doi.org/10.1111/j.1600-065X.2012.01131.x

Axtell, R.C., B.A. de Jong, K. Boniface, L.F. van der Voort, R. Bhat, P. De Sarno, R. Naves, M. Han, F. Zhong, J.G. Castellanos, et al. 2010. T helper type 1 and 17 cells determine efficacy of interferon-β in multiple sclerosis and experimental encephalomyelitis. *Nat. Med.* 16:406–412. http://dx.doi.org/10.1038/nm.2110

Axtell, R.C., C. Raman, and L. Steinman. 2011. Interferon-β exacerbates Th17-mediated inflammatory disease. *Trends Immunol.* 32:272–277. http://dx.doi.org/10.1016/j.it.2011.03.008

Axtell, R.C., C. Raman, and L. Steinman. 2013. Type I interferons: beneficial in Th1 and detrimental in Th17 autoimmunity. *Clin. Rev. Allergy Immunol.* 44:114–120. http://dx.doi.org/10.1007/s12016-011-8296-5

Azevedo, E.P., A.B. Guimarães-Costa, G.S. Torezani, C.A. Braga, F.L. Palhano, J.W. Kelly, E.M. Saraiva, and D. Foguel. 2012. Amyloid fibrils trigger the release of neutrophil extracellular traps (NETs), causing fibril fragmentation by NET-associated elastase. *J. Biol. Chem.* 287:37206–37218. http://dx.doi.org/10.1074/jbc.M112.369942

Calero, M., A. Rostagno, and J. Ghiso. 2012. Search for amyloid-binding proteins by affinity chromatography. *Methods Mol. Biol.* 849:213–223. http://dx.doi.org/10.1007/978-1-61779-551-0_15

Di Domizio, J., R. Zhang, L.J. Stagg, M. Gagea, M. Zhuo, J.E. Ladbury, and W. Cao. 2012. Binding with nucleic acids or glycosaminoglycans converts soluble protein oligomers to amyloid. *J. Biol. Chem.* 287:736–747. http://dx.doi.org/10.1074/jbc.M111.238477

Doherty, G.J., and H.T. McMahon. 2009. Mechanisms of endocytosis. *Annu. Rev. Biochem.* 78:857–902. http://dx.doi.org/10.1146/annurev.biochem.78.081307.110540

Eisenberg, D., and M. Jucker. 2012. The amyloid state of proteins in human diseases. *Cell.* 148:1188–1203. http://dx.doi.org/10.1016/j.cell.2012.02.022

Erlich, P., C. Dumestre-Pérard, W.L. Ling, C. Lemaire-Vieille, G. Schoehn, G.J. Arlaud, N.M. Thielens, J. Gagnon, and J.Y. Cesbron. 2010. Complement protein C1q forms a complex with cytotoxic prion protein oligomers. *J. Biol. Chem.* 285:19267–19276. http://dx.doi.org/10.1074/jbc.M109.071860

Goldschmidt, L., P.K. Teng, R. Riek, and D. Eisenberg. 2010. Identifying the amylome, proteins capable of forming amyloid-like fibrils. *Proc. Natl. Acad. Sci. USA.* 107:3487–3492. http://dx.doi.org/10.1073/pnas.0915166107

Gourdain, P., C. Ballerini, A.B. Nicot, and C. Carnaud. 2012. Exacerbation of experimental autoimmune encephalomyelitis in prion protein (PrPc)-null mice: evidence for a critical role of the central nervous system. *J. Neuroinflammation.* 9:25. http://dx.doi.org/10.1186/1742-2094-9-25

Grant, J.L., E.E. Ghosn, R.C. Axtell, K. Herges, H.F. Kuipers, N.S. Woodling, K. Andreasson, L.A. Herzenberg, L.A. Herzenberg, and L. Steinman. 2012. Reversal of paralysis and reduced inflammation from peripheral administration of β-amyloid in TH1 and TH17 versions of experimental autoimmune encephalomyelitis. *Sci. Transl. Med.* 4:145ra105. http://dx.doi.org/10.1126/scitranslmed.3004145

Hahm, B., M.J. Trifilo, E.I. Zuniga, and M.B. Oldstone. 2005. Viruses evade the immune system through type I interferon-mediated STAT2-dependent, but STAT1-independent, signaling. *Immunity.* 22:247–257. http://dx.doi.org/10.1016/j.immuni.2005.01.005

Hong, D.P., and A.L. Fink. 2005. Independent heterologous fibrillation of insulin and its B-chain peptide. *Biochemistry.* 44:16701–16709. http://dx.doi.org/10.1021/bi051658y

Hong, D.P., A. Ahmad, and A.L. Fink. 2006. Fibrillation of human insulin A and B chains. *Biochemistry.* 45:9342–9353. http://dx.doi.org/10.1021/bi0604936

Ji, Z., Z.J. Ke, and J.G. Geng. 2012. SAP suppresses the development of experimental autoimmune encephalomyelitis in C57BL/6 mice. *Immunol. Cell Biol.* 90:388–395. http://dx.doi.org/10.1038/icb.2011.51

Kurnellas, M.P., C.M. Adams, R.A. Sobel, L. Steinman, and J.B. Rothbard. 2013. Amyloid fibrils composed of hexameric peptides attenuate neuroinflammation. *Sci. Transl. Med.* 5:179ra42. http://dx.doi.org/10.1126/scitranslmed.3005681

Lande, R., D. Ganguly, V. Facchinetti, L. Frasca, C. Conrad, J. Gregorio, S. Meller, G. Chamilos, R. Sebasigari, V. Riccieri, et al. 2011. Neutrophils activate plasmacytoid dendritic cells by releasing self-DNA-peptide complexes in systemic lupus erythematosus. *Sci. Transl. Med.* 3:73ra19. http://dx.doi.org/10.1126/scitranslmed.3001180

López De La Paz, M., K. Goldie, J. Zurdo, E. Lacroix, C.M. Dobson, A. Hoenger, and L. Serrano. 2002. De novo designed peptide-based amyloid fibrils. *Proc. Natl. Acad. Sci. USA.* 99:16052–16057. http://dx.doi.org/10.1073/pnas.252340199

Matsubara, E., C. Soto, S. Governale, B. Frangione, and J. Ghiso. 1996. Apolipoprotein J and Alzheimer's amyloid beta solubility. *Biochem. J.* 316:671–679.

Narayan, P., S. Meehan, J.A. Carver, M.R. Wilson, C.M. Dobson, and D. Klenerman. 2012. Amyloid-β oligomers are sequestered by both intracellular and extracellular chaperones. *Biochemistry.* 51:9270–9276. http://dx.doi.org/10.1021/bi301277k

Nelson, R., M.R. Sawaya, M. Balbirnie, A.O. Madsen, C. Riekel, R. Grothe, and D. Eisenberg. 2005. Structure of the cross-β spine of amyloid-like fibrils. *Nature.* 435:773–778. http://dx.doi.org/10.1038/nature03680

Ousman, S.S., B.H. Tomooka, J.M. van Noort, E.F. Wawrousek, K.C. O'Connor, D.A. Hafler, R.A. Sobel, W.H. Robinson, and L. Steinman. 2007. Protective and therapeutic role for αB-crystallin in autoimmune demyelination. *Nature.* 448:474–479. http://dx.doi.org/10.1038/nature05935

Sawaya, M.R., S. Sambashivan, R. Nelson, M.I. Ivanova, S.A. Sievers, M.I. Apostol, M.J. Thompson, M. Balbirnie, J.J. Wiltzius, H.T. McFarlane, et al. 2007. Atomic structures of amyloid cross-β spines reveal varied steric zippers. *Nature.* 447:453–457. http://dx.doi.org/10.1038/nature05695

Scott, G.S., S.V. Spitsin, R.B. Kean, T. Mikheeva, H. Koprowski, and D.C. Hooper. 2002. Therapeutic intervention in experimental allergic encephalomyelitis by administration of uric acid precursors. *Proc. Natl. Acad. Sci. USA.* 99:16303–16308. http://dx.doi.org/10.1073/pnas.212645999

Serada, S., M. Fujimoto, M. Mihara, N. Koike, Y. Ohsugi, S. Nomura, H. Yoshida, T. Nishikawa, F. Terabe, T. Ohkawara, et al. 2008. IL-6 blockade inhibits the induction of myelin antigen-specific Th17 cells and Th1 cells in experimental autoimmune encephalomyelitis. *Proc. Natl. Acad. Sci. USA.* 105:9041–9046. http://dx.doi.org/10.1073/pnas.0802218105

Sheedy, F.J., A. Grebe, K.J. Rayner, P. Kalantari, B. Ramkhelawon, S.B. Carpenter, C.E. Becker, H.N. Ediriweera, A.E. Mullick, D.T. Golenbock, et al. 2013. CD36 coordinates NLRP3 inflammasome activation by facilitating intracellular nucleation of soluble ligands into particulate ligands in sterile inflammation. *Nat. Immunol.* 14:812–820. http://dx.doi.org/10.1038/ni.2639

Sjöberg, A.P., S. Nyström, P. Hammarström, and A.M. Blom. 2008. Native, amyloid fibrils and beta-oligomers of the C-terminal domain of human prion protein display differential activation of complement and bind C1q, factor H and C4b-binding protein directly. *Mol. Immunol.* 45:3213–3221. http://dx.doi.org/10.1016/j.molimm.2008.02.023

Sjölander, J., G.T. Westermark, E. Renström, and A.M. Blom. 2012. Islet amyloid polypeptide triggers limited complement activation and binds

complement inhibitor C4b-binding protein, which enhances fibril formation. *J. Biol. Chem.* 287:10824–10833. http://dx.doi.org/10.1074/jbc.M111.244285

Sokolowski, J.D., and J.W. Mandell. 2011. Phagocytic clearance in neurodegeneration. *Am. J. Pathol.* 178:1416–1428. http://dx.doi.org/10.1016/j.ajpath.2010.12.051

Weinger, J.G., P. Davies, C.M. Acker, C.F. Brosnan, V. Tsiperson, A. Bayewitz, and B. Shafit-Zagardo. 2012. Mice devoid of Tau have increased susceptibility to neuronal damage in myelin oligodendrocyte glycoprotein-induced experimental autoimmune encephalomyelitis. *J. Neuropathol. Exp. Neurol.* 71:422–433. http://dx.doi.org/10.1097/NEN.0b013e3182540d2e

Wender, P.A., D.J. Mitchell, K. Pattabiraman, E.T. Pelkey, L. Steinman, and J.B. Rothbard. 2000. The design, synthesis, and evaluation of molecules that enable or enhance cellular uptake: peptoid molecular transporters. *Proc. Natl. Acad. Sci. USA.* 97:13003–13008. http://dx.doi.org/10.1073/pnas.97.24.13003

Wiltzius, J.J., S.A. Sievers, M.R. Sawaya, D. Cascio, D. Popov, C. Riekel, and D. Eisenberg. 2008. Atomic structure of the cross-β spine of islet amyloid polypeptide (amylin). *Protein Sci.* 17:1467–1474. http://dx.doi.org/10.1110/ps.036509.108